385
10-18-78

Ai. 647

DOE/JPL/954854-3

PHASE 2 OF THE ARRAY AUTOMATED ASSEMBLY TASK FOR THE LOW COST SILICON SOLAR ARRAY PROJECT

MASTER

Third Quarterly Report

By
Manfred Wihl

MASTER

July 1978

Work Performed Under Contract No. NAS-7-100-954854

Solarex Corporation
Rockville, Maryland

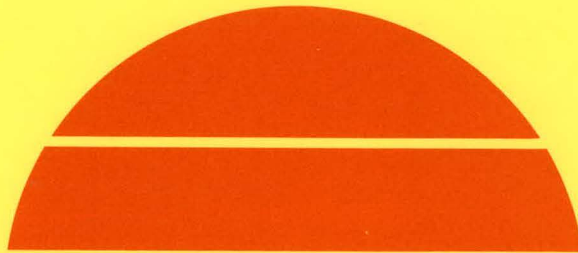

U.S. Department of Energy

DISTRIBUTION OF THIS DOCUMENT IS UNLIMITED

Solar Energy

DISCLAIMER

This report was prepared as an account of work sponsored by an agency of the United States Government. Neither the United States Government nor any agency Thereof, nor any of their employees, makes any warranty, express or implied, or assumes any legal liability or responsibility for the accuracy, completeness, or usefulness of any information, apparatus, product, or process disclosed, or represents that its use would not infringe privately owned rights. Reference herein to any specific commercial product, process, or service by trade name, trademark, manufacturer, or otherwise does not necessarily constitute or imply its endorsement, recommendation, or favoring by the United States Government or any agency thereof. The views and opinions of authors expressed herein do not necessarily state or reflect those of the United States Government or any agency thereof.

DISCLAIMER

Portions of this document may be illegible in electronic image products. Images are produced from the best available original document.

NOTICE

This report was prepared as an account of work sponsored by the United States Government. Neither the United States nor the United States Department of Energy, nor any of their employees, nor any of their contractors, subcontractors, or their employees, makes any warranty, express or implied, or assumes any legal liability or responsibility for the accuracy, completeness or usefulness of any information, apparatus, product or process disclosed, or represents that its use would not infringe privately owned rights.

This report has been reproduced directly from the best available copy.

Available from the National Technical Information Service, U. S. Department of Commerce, Springfield, Virginia 22161.

Price: Paper Copy $5.25
Microfiche $3.00

DOE/JPL/954854-3
Distribution Category UC-63b

PHASE 2 OF THE ARRAY AUTOMATED ASSEMBLY TASK FOR THE LOW COST SILICON SOLAR ARRAY PROJECT

THIRD QUARTERLY REPORT

NOTICE
This report was prepared as an account of work sponsored by the United States Government. Neither the United States nor the United States Department of Energy, nor any of their employees, nor any of their contractors, subcontractors, or their employees, makes any warranty, express or implied, or assumes any legal liability or responsibility for the accuracy, completeness or usefulness of any information, apparatus, product or process disclosed, or represents that its use would not infringe privately owned rights.

MANFRED WIHL

JULY 1978

Solarex Corporation

1335 Piccard Drive

Rockville, Maryland 20850

"The JPL low-cost Silicon Solar Array Project is sponsored by the U. S. Department of Energy and forms part of the Solar Photovoltaic Conversion Program to initiate a major effort toward the development of low-cost solar arrays. This work was performed for the Jet Propulsion Laboratory, California Institute of Technology by agreement between NASA and DOE.

DISTRIBUTION OF THIS DOCUMENT IS UNLIMITED

THIS PAGE

WAS INTENTIONALLY

LEFT BLANK

Table of Contents

1.	Introduction	1
2.	Metallization	3
2.1	Requirements of a Contact Metallization System	3
2.2	Process Sequence	6
	2.2.1 Vacuum Deposition	7
	2.2.2 Positive Silk Screening	8
	2.2.3 Negative Silk Screening	9
2.3	Verification of Metallization	11
	2.3.1 Contact Adhesion	11
	2.3.2 The Nickel/Silicon Interface	16
	2.3.3 Series Resistance and Shadowing	18
	2.3.4 Resist Ink and Line Width	26
	2.3.5 Economic Analysis	28
3.	Junction Formation, Quantum Yield	31
4.	Interconnection and Encapsulation	33
4.1	Review and Assessment of Interconnection Encapsulation	33
4.2	Verification Experiments	36
	4.2.1 Arc-Spraying	36
	4.2.2 Laminating	41
	4.2.3 Parallel Gap Welding	42
5.	Conclusions	47
6.	Recommendations	47
7.	New Technology	47

List of Tables

2.3.1.1	Pull Strength of Wave Soldered Cells at 45°	14
2.3.1.2	Pull Strength at 90°	15
2.3.5.1	Cost of Metallization Steps	30
4.2.2.1	Lamination Materials and Characteristics	43
4.2.3.1	Parallel Gap Welding Pull Strength Results at 45°	45

List of Figures

2.3.2.1	Nickel Sintering	17
2.3.2.2. A,B, & C	Photographs of Silicon/Nickel Interface	19,20
2.3.3.1	Textured, Wave Soldered Solar Cell	21
2.3.3.2	Metallization Pattern	21
2.3.3.3	Cell Efficiency, 100 Ω/□ Sheet Resistance	24
2.3.3.4	Cell Efficiency, 50 Ω/□ Sheet Resistance	25
3.1.1	Quantum Yield for Textured Cell	32
4.1.4.1	Conceptual Arrangement of Cell Interconnection	37
4.2.1.1	Photograph of Arc-Sprayed Tab	40
4.2.1.2	Photograph of Arc-Sprayed Tab	40
4.2.3.1	Parallel Gap Welding Pull Strength Results Summary	46

1. INTRODUCTION

This third quarterly report documents the results of the continuing work done on the feasibility of manufacturing photovoltaic solar modules in a future automated production facility. During this quarter we completed the verification of metallization, and junction formation, and started the verification of interconnection and encapsulation of cells into modules.

The metallization of 4" silicon wafers can be efficiently done using negative silk screening, electroless nickel plating, and wave soldering. After reviewing other possible metallization schemes this particular combination of processes has shown great promise for automation and cost effectiveness. Various verification experiments have been performed to indicate its reliability and manufacturing efficiency. The results of pull strength tests conducted on the cell interconnects demonstrated the excellent adhesion properties of the metallized layer. In addition, prolonged exposure to humidity and high temperature had no perceptable effect on the visual or electrical performance of the cells. Special emphasis was placed on the nickel/silicon interface. The results presented in this report show no visual evidence of nickel spiking through the p-n junction. Another topic described, deals with a computer assisted study which has given new insight into the effects of line width and thickness of the metallization grid on the solar cell efficiency. Final economic analysis of the metallization step was also performed showing that the total cost of materials and equipment could be about 17¢ per wafer.

Verification of the final process step of this contract, consisting of interconnection and encapsulation, was begun during this quarter. Thus far, arc-spraying contacts onto glass has been successfully achieved using an aluminum/copper double metal layer combination. In addition, experimentation with

various laminating substances has already identified three types of plastics which have shown good promise of securing the cells.

Parallel gap welding has also been developed to the point of achieving excellent and consistent results of contact adhesion. Tabs connected with the technique proved to be very reliable.

In summary, all of the processes described within this report were choosen for verification by Solarex in an attempt to minimize the cost of producing solar modules by eliminating the use of inherently expensive materials and by utilizing future automated technologies. Most importantly, the overall cost of the automated process appears to be within the 50¢ per watt of desired cost which demonstrates the feasibility of achieving the national goal.

2. Metallization

2.1 Requirements of A Contact Metallization System

The metal contacts of a solar cell must meet electrical, physical and economic requirements. Specifically, the contacts must have low series resistance with minimum shadowing, firm adhesion to the silicon, enviromental stability and must form an ohmic electrical interface, as well as cost only a few cents per watt under automated manufacture. The importance of these requirements shall be reviewed.

For front surface metallization there is a trade-off between series resistance and shadowing. In order to reduce the series resistance to an acceptable level the shadowing is often more than 10% of the cell area when solder is used as the conductor. Series resistance has two components, resistance through the metal line and sheet resistance through the diffused silicon. Reducing either component will increase shadowing. For example, line resistance is reduced by widening the line and sheet resistance is reduced by increasing the number of lines per centimeter. Our verification work includes a mathematical analysis of the series resistance components versus shadowing in order to identify the contact geometry of minimum power loss and to quantify the magnitude of losses that can be expected.

The second requirement is that the metal contacts adhere to the front and back of the cell for the entire life of the solar panel. Over most of the cell surface adhesion needs to be sufficient to maintain good electrical contact. Around the interconnections there is potentially additional stress from the cell tab. This stress is difficult to quantify since making direct measurements inside the panel is virtually impossible. Nevertheless, a level of acceptance has been

derived indirectly. In 1977 JPL purchased and deployed a large number of panels for which sample cells underwent a 90° "pull test" with the passing criteria of 167 grams tension without tab failure. These panels have proven to be reliable in the field. Currently, JPL is using arbitrarily 225 grams as the criterion for passing. Using this arbitrary criterion our nickel-solder metallization system exceeds the test since the 90° pull strength of tabs soldered to the front and the back are both typically in excess of 250 grams.

The requirement of environmental stability of the contacts is of utmost importance since for a fixed manufacturing cost the cents per kilowatt-hour of photovoltaic power depends on the operational life of the panel. Accelerated enviromental testing has been used to verify that our proposed metallization system does not degrade under temperature cycling and high humidity.

The fourth requirement is that the metal/silicon interface be ohmic. An abrupt metal/silicon interface will form a Schottky barrier that reduces the output voltage. This barrier can be eliminated by sintering to form an ohmic contact. Sintering involves heating the wafer so that some of the contact metal, nickel in this case, diffuses into the silicon forming Ni_2 Si and NiSi. The nickel diffusion and chemical formation of nickel silicide enhances the adhesion, as well as forming an ohmic contact.

There has been concern that the nickel would diffuse into the junction region, degrading cell performance. Sintering experiments have been done to quantitatively define the nickel diffusion process. From these experiments a time and temperature window has been found for which cell performance is not degraded yet good adhesion is assured and an ohmic contact is created.

The final requirement is that the metallization step be of low cost, a fraction of the total cost goal of 50¢ per watt. In addition, the volume of production must be able to meet the goal of 500 MW-pk annual production. If a single production line is to process one tenth this amount in a 24 hour operation the rate should be about 120 4" wafers per minute. Our analysis indicates that this rate of production is possible with our proposed metallization technique. Furthermore, an economic analysis has been carried out which indicates that the cost for this step is a few cents per watt.

Before giving details of our verification experiments and cost analysis our proposed metallization sequence will be described and compared to the conventional techniques.

2.2 Product Sequence

After junction formation it is necessary to metallize the front and back of the solar cell in order to collect and conduct all of the current to the external circuit. The techniques currently in use are vacuum deposition using a shadow mask or photolithography, positive silk screening and negative silk screening. Solarex's negative silk screening process is inherently low in cost and can be easily adapted to an automated sequence. The other processes, in contrast, are plagued by either special handling requirements, low levels of reproducibility, overall high cost, or poor interface qualities with the adjacent step. In addition, they require high energy expenditure, large equipment investment, batch processing, and time delays.

This section will briefly review each deposition technique and demonstrate why negative silk screening avoids the difficulties created by the other processes. Solarex's complete metallization sequence involves three simple steps each utilizing a machine that can be easily modified to a belt system. The proposed negative silk screening metallization technique consist of: 1) negative silk screening, 2) electroless nickel plating, and 3) wave solder dipping. In the negative silk screening step the resist ink will be applied in such a way that only that portion of the silicon which will be metallized is left exposed. The cells are then passed through an electroless nickel plating bath which deposits the nickel and thus forms the metal/silicon interface. After removing the resist ink the conductivity is enhanced by being dipped in a pool of solder. The solder will only

adhere to nickel and thus the pattern is complete. The results have shown that this metallization technique satisfies the criteria for good contacts, and can easily be interfaced in the overall automatic process sequence. The technique will eliminate the high cost of photosensitive polymers, increase process reliability and still maintain the effectiveness of silk screening. Most importantly, the process is a continuous flow system with no inherent delays in the overall operation.

2.2.1 Vacuum Deposition

In order to compare the various contact metallization techniques the principal features of each technique will be reviewed beginning with the two vacuum methods, shadow masking and photolithography.

Shadow Masking

There are primarily two methods of delineating the contact pattern on solar cells within a vacuum: shadow masking and photolithography. Shadow masking, as the name implies, involves covering the front of the cell with a metal mask that leaves the desired pattern exposed. Under vacuum a single metal or a system of metal layers is evaporated onto the exposed silicon surface.

The high energy requirements and large waste of evaporated metal tends to lower the possibility of using shadow masking as a potential candidate for an automated sequence. A great deal of energy is used in achieving and maintaining a high vacuum for the entire process to occur. For example, a vacuum system capable of processing 140 cells per hour requires a diffusion pump that uses 1900 watts continuously. This is over 13 W-hours per wafer for pumping alone. The evaporation of metal will add several more kilowatts to the

total energy per wafer. Furthermore, a large percentage of the evaporated metal is lost because the metal coats the entire chamber while only a small portion is deposited on the exposed silicon. Recycling the metal deposited on unwanted surfaces constitutes an additional expense. The use of conventional evaporation systems are not practical for an automated future line due to the cost and amount of waste that is part of the process.

Photolithography

The photolithographic process is a multi-step metallization technique which includes vacuum deposition and two baking cycles. As a first step, a layer of metal is deposited on the entire wafer. Then a pattern of photo-sensitive resist is exposed onto this layer. The excess metal can be etched away and leave the wafer with a metal inter-connection pattern.

The photolithographic process is a good method of providing high resolution and high quality patterns. It is an excellent technique for producing cells with fine line patterns used extensively in concentrator systems. This high level of sophistication, however, is not needed in our development of automation cells. Fine lines are not necessary nor desired for these wafers, in fact, wider lines provide better adhesion. Most importantly, our scheme of negative silk screening represents a basic technology and avoids the capital investment of vacuum systems.

2.2.2 Positive Silk Screening

In contrast to vacuum deposition, silk screening is a very attractive method of metallizing solar cells. Machines exist which can print at the rate equivalent to the area of 120 4" wafers per minute. There is no need for a vacuum or time consuming processes such as spinning exposing, de-

veloping and baking which slow down the process or demand high energy input. In addition, the process can be easily adapted to automation.

A metallized pattern can be printed directly onto the surface of the wafer. The process involves printing a metallized "ink" directly through a contact pattern stencil attached to a thread mesh. The "ink" consists of a very fine metal powder mixed with a liquid vehicle and glass frit. The glass aids in adhesion to the silicon surface. The ink must be baked above the melting point of the glass frit. Due to the different expansion coefficients of each substance a careful control of cooling time and ink composition is necessary.

Work done within the industry, has demonstrated reliability problems with the process. In a real environment the metallization layer did not survive well on the silicon.

Also, the cost of positive silk screening has determined that it is impractical for our application. The metallizing substance is the main expense which comes approximately to $0.26/watt definitely out of range for the national goal.

2.2.3 Negative Silk Screening

In view of the advantages of silk screening, simplicity, but high cost, Solarex has developed a specific technique called "negative" silk screening which eliminates the use of high cost metal based inks. The silk screeining is used to apply a negative print of the desired pattern on the cell using a very inexpensive resist such as polyurethane. This leaves the wafer ready for subsequent metal coating in an electroless nickel plating solution.

The nickel will only adhere to the bare silicon or, in other words, the desired grid pattern. Once the wafer is plated, the polymer coating is dissolved with an organic agent leaving only the nickel line pattern. The nickel layer is yet too thin, however, for proper cell operation. To increase the line thickness the entire cell is dipped into a solder bath where the solder will only adhere to the nickel layer on both the front and back contacts. This provides a good means of conducting current and interconnecting cells.

This particular process, which does not require an impressed electric potential, is much simpler than electrolytic plating. Electrolytic plating requires individually securing each cell to the electrodes on a rack. The racks are placed in the plating solution and current is passed through them. Plating thus becomes a batch type process which drastically reduces the throughput rate of the system. Electroless nickel plating, in contrast, requires no special handling and does not require a power supply. A system can easily be devised which carries cells through the bath at a constant rate.

Solder coating is also an effective technique which is widely used in related industries and can be easily modified to automatically solder coat solar cells. For example, wave solder machine manufacturers have facilities to reliably coat a continuous flow of printed circuit boards. By substituting solar cells for PC boards the complete solder dipping step can be accomplished by one machine.

Experiments have shown that this procedure can effectively meet the requirements of contact adhesion, enviromental stability and cost effectiveness. The pull tests performed on sample cells compare favorably with those of the vacuum based metallization procedure. The silicon/nickel interface has not only shown excellent contact adhesion, but after prolonged exposure (1 month) to humidity and temperature (90° relative humidity, 70^{0} C) there was no perceptable difference in visual or electrical characteristics of the cell.

In summary, the simplicity and use of inexpensive materials has made Solarex's negative silk screening an effective and inexpensive metallization technique for future automation.

The verification work done to demonstrate the viability of this process is detailed in the next section.

2.3 Verification of Metallization

2.3.1 Contact Adhesion

Contact adhesion has been the object of concentrated efforts over the last quarter. The importance of contact adhesion becomes apparent when one considers the future stresses the solar cell will encounter. In an automated process the cells are moved quickly from station to station being shifted constantly making the contacts vulnerable to scrapping. Also, once encapsulated the cell experiences stresses caused by changing enviromental conditions. Wafers are stressed from contraction and expansion of the panel caused by temperature changes and mechanical loading such as wind forces. The results presented in this section indicate that the automation cells can withstand this type of pressure.

Traditionally, the nickel/silicon interface has not been considered reliable. The difficulty occurs in determining the exact parameters of nickel sintering..Under high temperatures and long exposure times the nickel will diffuse

through the p-n junction of the solar cell. Solarex has done extensive work on defining the temperature and duration of nickel sintering. The outcome of this work has produced parameters with which good contact adhesion are obtained without affecting the junction characteristics. This is proven by the results obtained in pull strength experiments.

The results of pull strength tests done on wave soldered cells are listed in Table 2.3.1.1 and 2.3.1.2. According to different criteria for the measurement of contact adhesion two pull angles were used. Tabs pulled at 45° are in accordance with Air Force specifications and tabs pulled at 90° follow JPL procedures for flat plate panels.

In Table 2.3.1.1 the results of pull strength tests performed on wave solder cells are presented. The tests follow the Air Force specification for space cells (MIL-C-83443A) of a 45° pull angle and 250 gram minimum passing requirement. It can be seen that the mean pull strength (1163 grams) exceed the Air Force specifications by almost a factor of five.

Another set of pull strength tests (Table 2.3.1.2) were performed in which the tabs are pulled at 90°. One can see that the mean pull strength of the wave soldered cells (285 grams) easily satisfies the 225 gram passing requirement for JPL flat plate panels. The results of average pull strength of vacuum metallized cells are presented for comparison.

There was no consistent point of failure; the solder/nickel interface ruptured as often as the nickel/silicon interface. Hence the nickel/silicon interface is as strong as the solder/nickel interface. This demonstrates the good adhesion properties of the nickel/silicon interface.

Several samples of cells processed using the wave solder technology were tested in the Solarex humidity chamber. The tests lasted over a month at 90% relative humidity and at 72° C temperature. All cells were tested carefully every few days to detect any degradation in cell characteristics: No degradation was observed.

PULL STRENGTH OF WAVE SOLDERED CELLS AT 45°

SAMPLE #	PULL STRENGTH (grams)
1	1274
2	1415
3	1387
4	1415
5	905
6	1415
7	1174
8	1104
9	849
10	1330
11	849
12	1132
13	1302
14	1358
15	905
16	1188
17	1132
18	1358
19	1018
20	933
21	1387
22	1245
23	679
24	1019
25	1302

MEAN PULL STRENGTH:

1163 grams

TABLE 2.3.1.1

PULL STRENGTH AT 90°

SAMPLE #	WAVE SOLDERED (grams)	SAMPLE #	VACUUM (grams) METALLIZATION(Ti-Ag)
12	799	1	317
8	397	2	340
88	170	3	416
10	227	4	408
15	198	5	262
14	17	6	378
13	85	7	316
25	284	8	338
19	510	9	354
20	255	10	370
24	198	11	374

MEAN PULL STRENGTH	MEAN PULL STRENGTH
285	352

TABLE 2.3.1.2

2.3.2 The Silicon/Nickel Interface.

The boundary between the solder contact and the silicon is bridged by a layer of nickel. The nickel is deposited using electroless plating after which it must be sintered. The sintering step has two effects, it eliminates the Schottky barrier and it enhances adhesion. Though nickel contacts have been generally used in the photovoltaic industry there has been much discussion of nickel contact realiability especially with the shallow junctions found in solar cells. Indeed, nickel diffuses into silicon relatively fast at elevated temperatures and can degrade cell performance. However, the rate of nickel diffusion changes with temperature and therefore can be controlled.

We have looked for a "window" of sintering time and temperature for which nickel adhesion is assured yet the nickel does not diffuse to the junction depth.

Figure 2.3.2.1 summarizes the results of initial sintering experiments done at Solarex. In these experiments cells were heated to a pre-determined temperatures for a minute then moved to a test station. After being measured the cells were again heated for a minute, and so on. The measurement most sensitive to the diffusion of nickel is the leakage current, which is the measure plotted in Figure 2.3.2.1. Actually, not all cells began with an initial value of 2 mA leakage at 300 mV, this plot is an average of many cells.

The temperature dependence of nickel diffusion shows up very clearly on the graph. At 450°C the cell is significantly degraded within two minutes while virtually no change occurs in thirty minutes at 250°C. We have found that nickel adhesion is assured when sintering at 350°C for one minute. Our experiments indicate that under these sintering conditions the increase in reverse dark current amounts to less than 5%. The effect on

Figure 2.3.2.1 Nickel Sintering

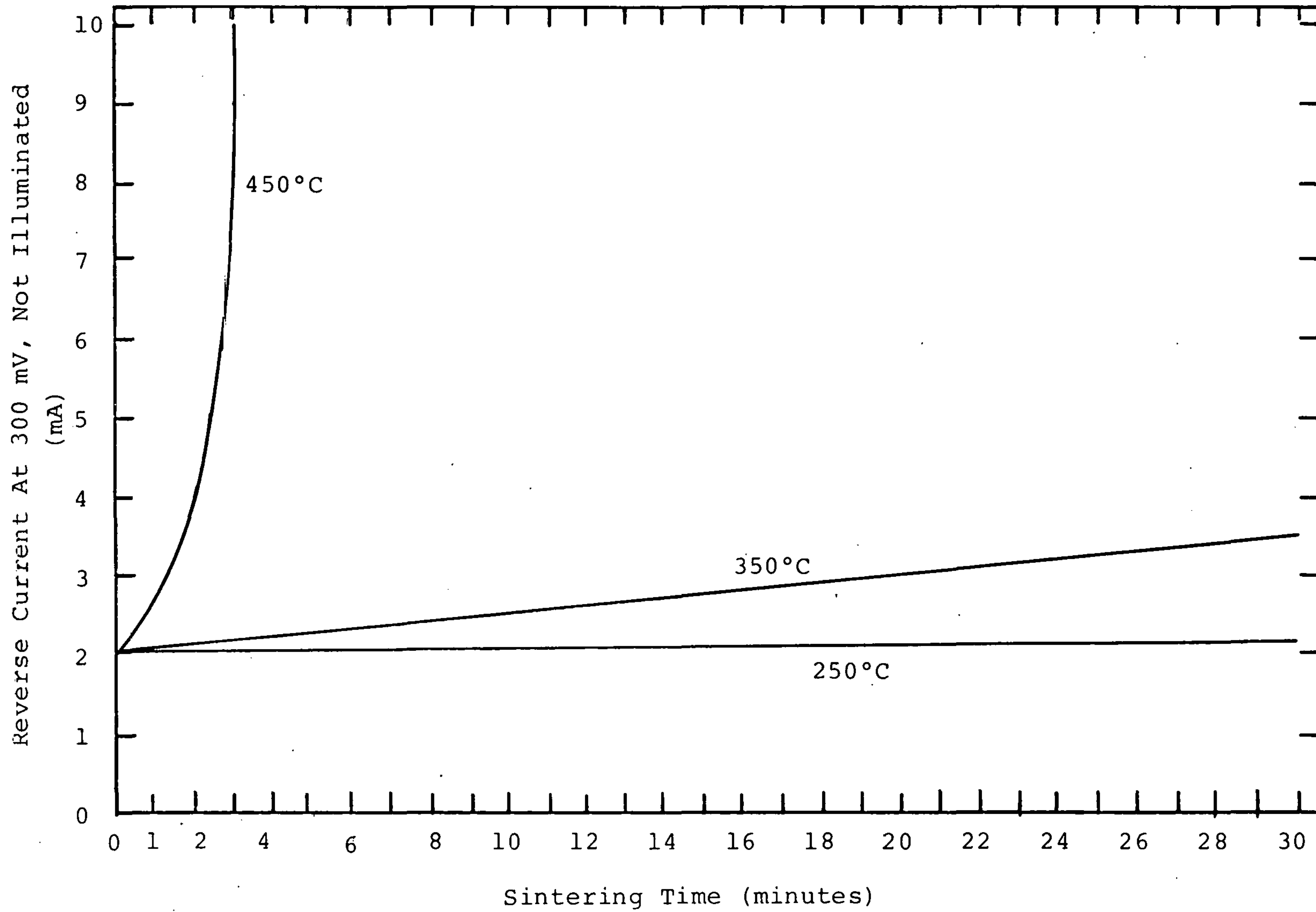

the output power was found to be less than 1.% reduction.

We have also studied the silicon/nickel interface optically, using the angle lapping technique. By angle lapping at 3° from the surface plane, shallow features can be stretched so that a depth of one micrometer appears on the surface with a width of 19 micrometers. Even with this technique it is difficult to image features as shallow as the diffused region, 0.5 micrometer deep. At 118 magnification the junction will appear on the picture as $0.5 \times 10^{-6} \times 19 \times 118 = 1.1$ millimeters. Hence, we did not expect to reveal the actual diffusion of nickel. We had already verified from electrical measurements that the nickel does not diffuse through the junction specific sintering conditions. We were looking for effects other than simple diffusion, i.e. spiking or motion along dislocation. Figures 2.3.2.2.A,B, and C show no evidence of either phenomenon.

2.3.3 Series Resistent and Shadowing.

There are three major, unavoidable sources of power loss that are influenced by the metallization geometry. There is the voltage drop across the conducting lines of the pattern, a voltage drop across the thin diffused region, and shadowing since the metal lines are opaque. Any one of these loss mechanisms cannot be eliminated without increasing another.

The situation is best illustrated by deriving the mathematical equations of power loss for a simple pattern, as shown in Figure 2.3.3.1. From the equations the ideal line width and spacing between lines can be derived. This in turn indicates the printing resoltuion required and the amount of power loss that is unavoidable. Though the results are based on a simple pattern our extensive experience in designing contact patterns has taught us that the ideal line width and spacing for a sophisticated, optimized pattern will not be significantly different.

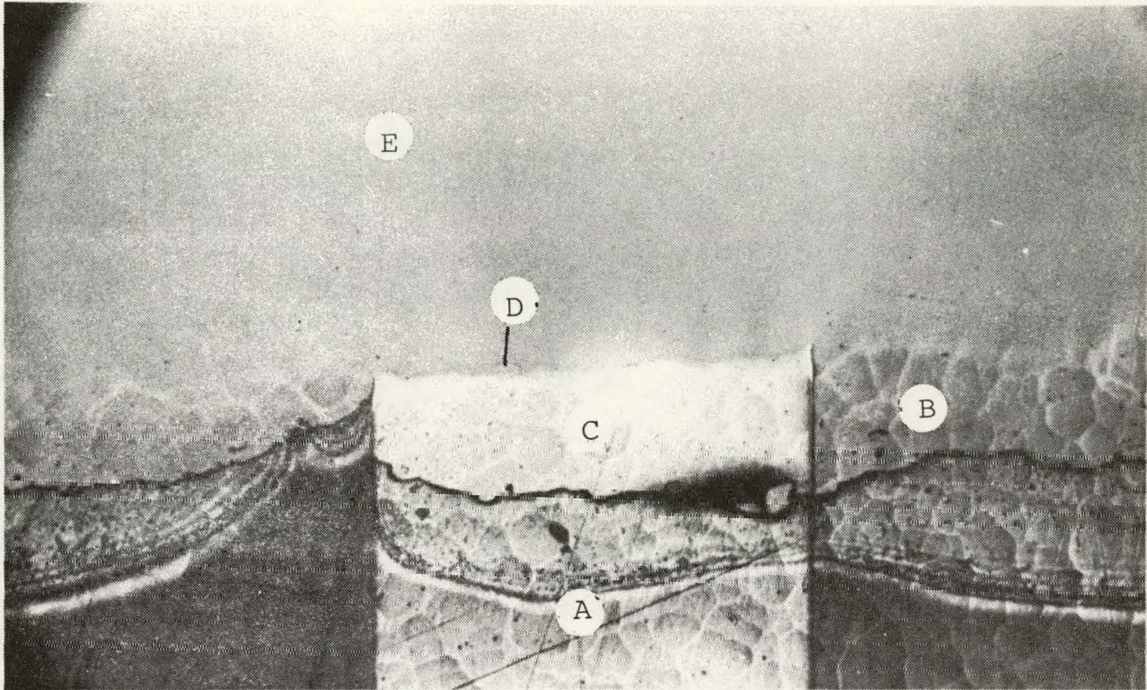

Figure 2.3.2.2.A

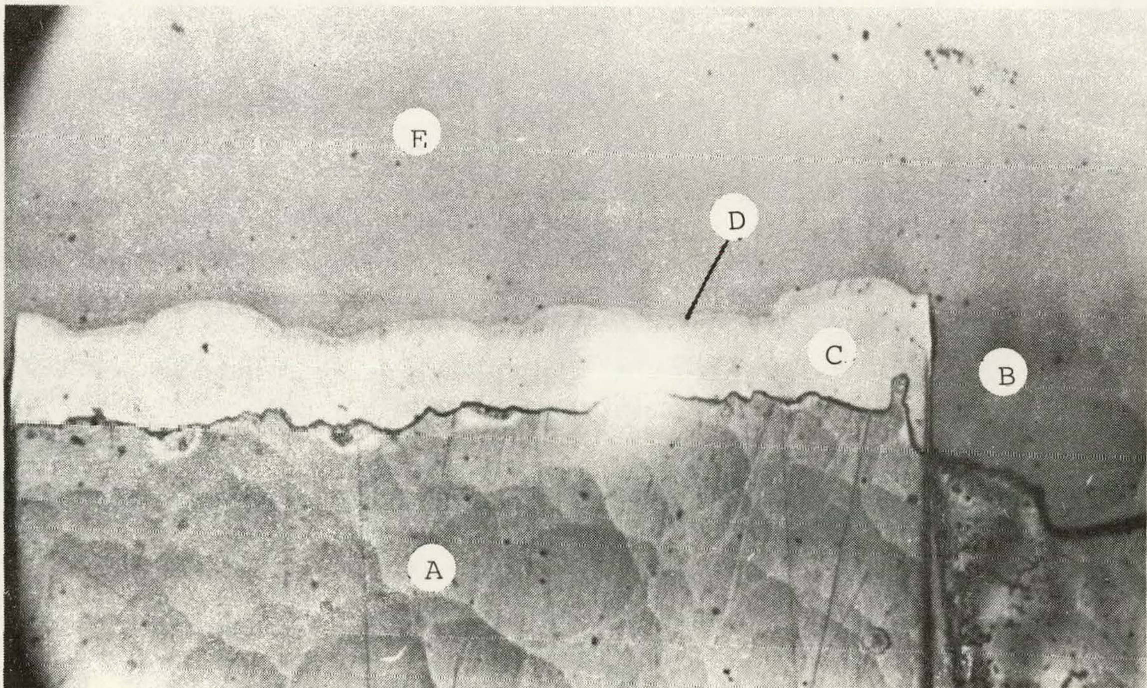

Figure 2.3.2.2.B

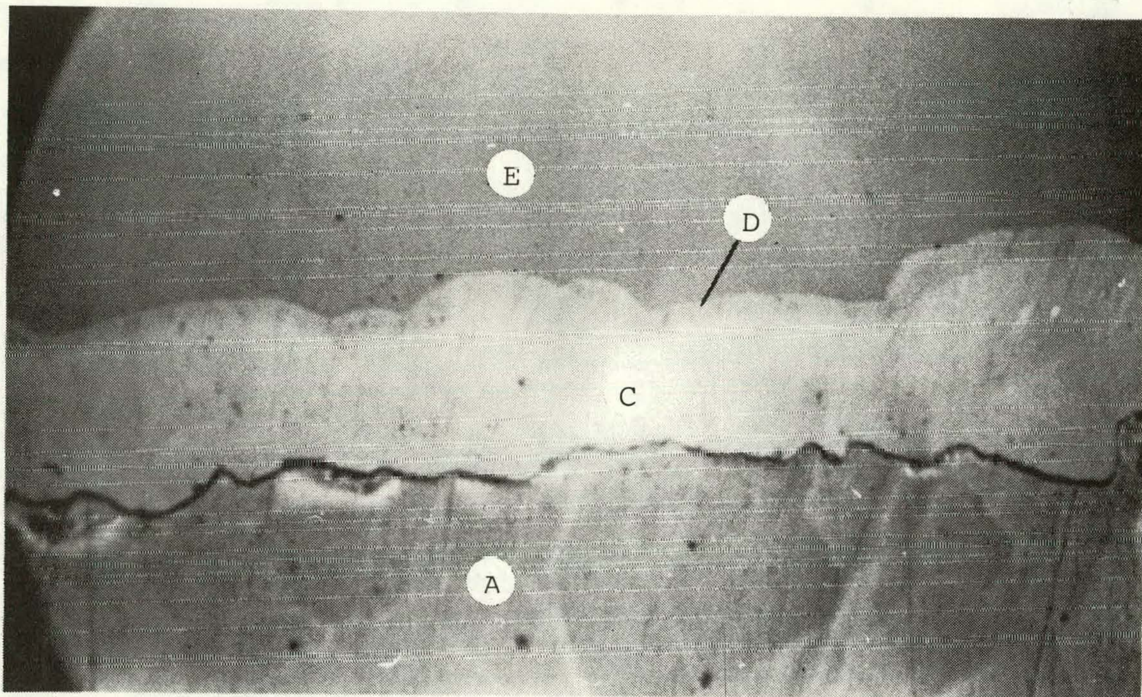

Figure 2.3.2.2.C

Figure 2.3.2.2.A	Nickel Contact Sintered At 350°C, 1 min.,	30X
Figure 2.3.2.2.B	Nickel Contact Sintered At 350°C, 1 min.,	59X
Figure 2.3.2.2.C	Nickel Contact Sintered At 350°C, 1 min.,	118X

Key to regions in pictures

a) Plastic used for imbedding sample

b) Silicon surface exposed through torn plastic. ("pillowed" by alkaline etch)

c) Nickel surface

d) Angle lapped nickel

e) Angle lapped silicon

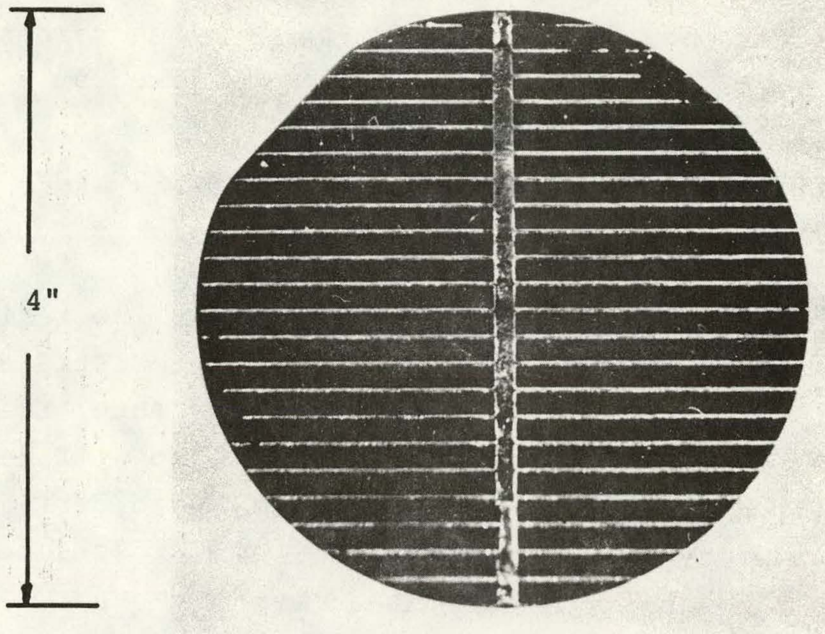

Textured, Wave Soldered Solar Cell

Figure 2.3.3.1

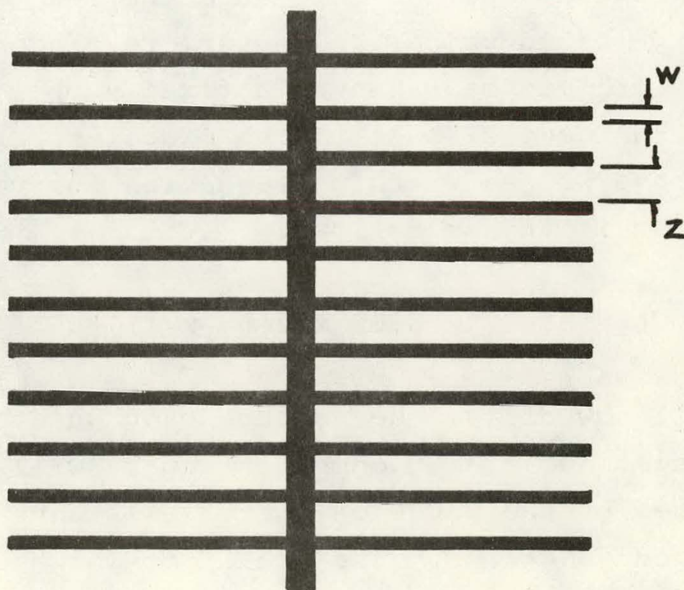

Metallization Pattern

Figure 2.3.3.2

The calculations are based on a 10.16 cm (4 inch) diameter cell with a central buss and a uniform set of lines perpendicular to the central buss. The central buss will be fixed at a width of 2mm, which gives 2% shadowing and a negligible series resistance. The variables will be the line width, w, and the distance between lines, z. (See Figure 2.3.3.2).

Let us first derive the voltage drop due to line resistance. The resistance, R, is the product of the solder resistivity, ρ, (15×10^{-6} Ω-cm) times the length of the current path, L, divided by the cross-section, A ($R = \rho \frac{L}{A}$). A wider line will be greater in height as well due to the solder meniscus formed during the dipping process. To represent this phenomenon the cross-section is approximated by a square.

The voltage drop in the line is the resistance multiplied by the current. The current, in turn, is the product of the area surrounding the line, 5.08 x z, times the current generation density, about 0.032 A/cm^2. Recall that the resistance depends on the length of the current path. Since current generated near the central buss will flow a shorter distance through the line than current generated near the cell edge the length of the current path is not a fixed number. However, to a good approximation the line length can be taken as a fixed number, 2.54 cm, the distance from the central buss to the midpoint. From the above considerations we can write the equation for voltage drop in the line, calling it VL, as follows.

$$VL = (.032 \times 5.08 \times 2.54 \times z) / w^2$$

We will now derive the voltage drop due to sheet resistance. A sheet resistance of 100 ohms per square will be used since this is the center of the range of sheet resistance that are correlated with good junctions. The area from which current flows into a line can be divided into parallel squares of area $(z/2)^2$. Actually, the average current goes half the length of the square so the resistance will be taken as 50 ohms. The voltage drop in the

diffused sheet, which will be called VS, can be written as follows.

$$VS = (R_{sheet}/2)\ (.032)\ (z/2)^2$$

The fractional power loss due to both voltage drops can be written

$$(VL + VS)/.45$$

where 450 mV is the usual operating voltage at the peak power point.

When the initial efficiency includes the central buss shadowing the fractional power drop due to current reduction from shadowing by the perpendicular lines can be written as w/z.

In summary, an initial efficiency is assumed which is the then derated by the fractional voltage drop and the fractional shadowing. The initial efficiency includes the loss from the central buss, about 2% shadowing, since this value is held fixed. The final efficiency, EFF, can be derived from combining the previous equations.

$$EFF\ (w,z) = (1-w/z) \times (1 - \frac{VL + VS)}{.45} \times \text{Initial Efficiency}$$

A computer program was used to solve this equation for a matrix of w and z values. The output is graphed in Figures 2.3.3.3 and 2.3.3.4. The initial efficiency is taken as 15%. The choice for initial efficiency is not critical, a different choice would shift the position of the topographic lines but would not change the shape nor move the point of maximum efficiency.

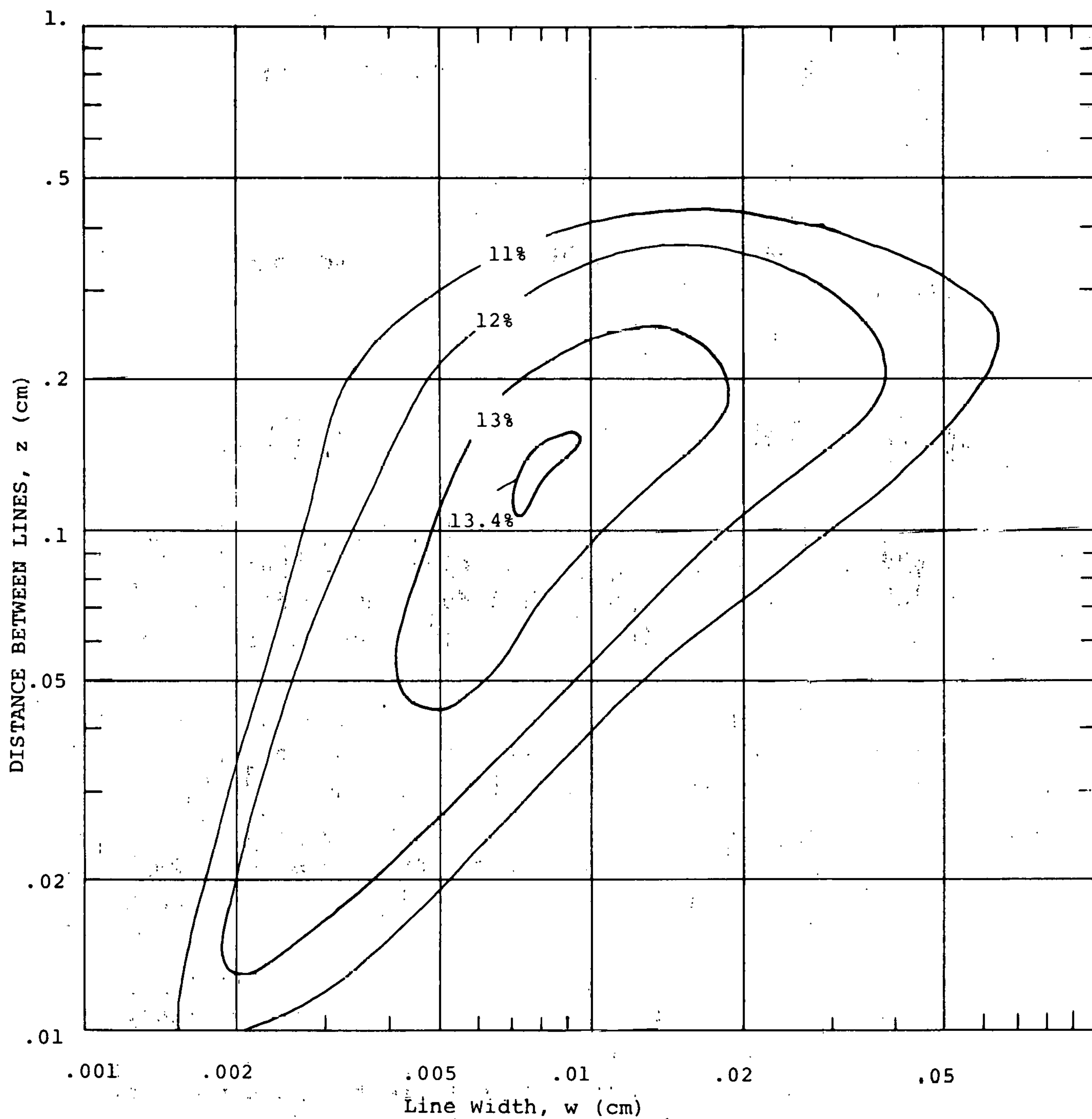

FIGURE 2.3.3.3 EFFICIENCY, 100 Ω/□ SHEET RESISTANCE

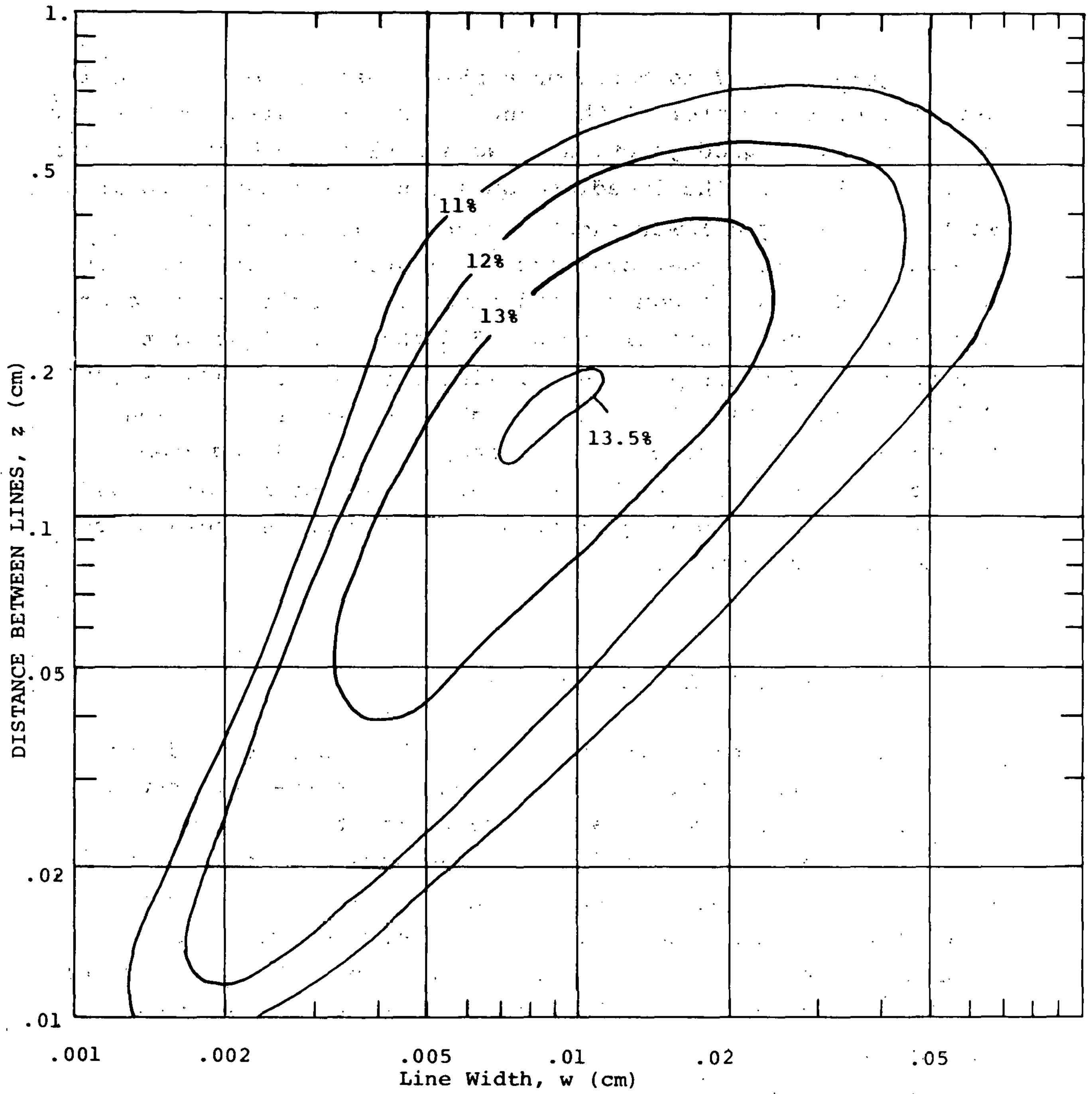

FIGURE 2.3.3.4 EFFICIENCY 50Ω/□ SHEET RESISTANCE

Figure 2.3.3.4 is based on a sheet resistance of 100 ohms per square, the center of the range of sheet resistance that are correlated with good junctions. We see that the best final efficiency is 13.4%. The immediate question is whether it would be worth generating a lower sheet resistance in order to reduce the number of lines per centimeter. Figure 2.3.3.4, which is based on 50 ohms per square, indicates that a slight improvement can be obtained. From figure 2.3.3.3 the ideal line width can be found for 100 Ω/□ sheet resistance, about .0027" - .0035". This is a resolution that can be achieved with silk screen printing. If 13% efficiency is accepted with 50Ω /□ sheet resistance the lines can be as wide as 240 microns, or .0094". We are currently working on obtaining silk screen resolutions on the order of 9 mils.

2.3.4 Resist Inks and Line Widths

The search for different resist inks has continued over the last quarter. The last report on silk screening stated the polyurethane varnish was the most effective ink found. After some work with four inks from Advance Screen Printing Company the polyurethane remains the best material we could identify. Polyurathane will extrude easily through the screen and yet hold the pattern once applied. It holds up well in the electroless nickel bath and is easily removed with an organic agent.

The four new inks are presented below:

SAMPLE	CODE NUMBER	RESULTS
1	R 918413	This blue ink clogs the screen quickly (approximately every 10 wafers) because of its quick drying property. Cleaning solutions do not open the screen. The material holds up in the Ni solution although it does not lift off very well. The solvent

Sample	Code Number	Results
1 (cont.)	R 918413	merely dilutes the resist and does not slough off.
2	R 97E	Brown resist does not screen smoothly leaving sections uncovered. The Ni bath will ruin the pattern at operating temperatures. This is probably a matter of a few degrees centigrade.
3	R 511-5B	Black resist worked well in printing solid or fine lines It was inconsistent, however, in the Ni bath giving random results.
4	R 918-413 and R 511-5B	Samples 1 and 3 were mixed together in the hope of using the favorable properties of each. The combination worked well in screening and Ni resistence. Clogging of the screen, however, remains a problem.

It was found that Xylol is the best general solvent for removing the resists. The fibers of the polyester screen were beginning to show degradation after being cleaned with acetone. This can be eliminated by using a stainless steel screen.

Line Widths:

The results of the computer programs, presented in the previous section, showed that the line width should be no greater than 9 mils. Though this may be considered hard to achieve we are currently working towards this goal. A trade-off occurs, however, between the line width and the desired

cell efficiency. Figure 2.3.3.4 shows that by relaxing the criteria of efficiency by 0.5%, line width can be increased by 3.9 mils (0.01 cm). Wider lines are, in fact, desireable for greater contact adhesion and ease of silk screening. Thus far, resist inks have been used which yield resolutions of 24 and 18 mils which should yield cell efficiencies of 12%.

2.3.5 Economic Analysis of Metallization

The three steps of metallization, silk screening, nickel plating, and solder dipping, are estimated to cost 17¢ per 4" wafer. This is within the budget of 50¢/wafer for the entire process.

A specific breakdown of costs will be provided below. In several areas the numbers differ from the preliminary analysis provided in Solarex's second quarterly report. The revisions are due to additional information obtained subsequent to the last report.

2.3.5.1 Silk Screening

A large area, high through-put rate precision silk screening machine costs about $5,000. When the cost of wafer handling equipment is included the total equipment cost is expected to be $8,000. Since about six wafers can be printed in a single six second cycle one machine can print over 25 million wafers per year. Amortized over a three year period the cost of equipment will be 0.01¢/wafer. The major cost will be resist ink since about 85% of the wafer area is covered. A four liter jar of urethane based resist at $20/jar prints about 1,000 wafers for a cost of 2¢/wafer. Furthermore, a $50. screen and stencil will last for at least 1,000 print cycles yielding a cost of 0.8¢/wafer. One operator

will be required to replace screens and maintain mechanical tolerances for a labor and overhead cost of approximately 3¢/wafer for two shifts. In sum, the cost will be about 6¢/wafer.

2.3.5.2 Electroless Nickel Plating

Nickel plating involves immersion of the wafer into a plating solution. In order to process one tenth of the national goal, 120 wafers must be processed each minute. Since plating requires ten minutes about 1,200 wafers must be immersed at any one time. The volume of liquid can be minimized by placing the wafers close together, for example, by using several slowly rotating carrousels submerged in the plating solution. Each carrousel would have several hundred vertical slots. The equipment cost is estimated to be $20,000. Amortized over three years this is about 0.02¢/wafer. The electroless nickel plating solution costs about $1.20/liter and one liter will plate 250 4" wafers yielding a materials cost of 0.5¢/wafer. One operator will be involved in monitoring the equipment and mixing chemicals. The total cost for this step, including overhead, is expected to be 4¢/wafer.

2.3.5.3 Wave Soldering

Wave soldering equipment capable of coating 120 wafers per minute is expected to cost $40,000. Amortized over three years this is 0.03¢/wafer. The solder costs 10.3¢/cc for 60-40 composition. The thickness on the wafer is about 50 micrometers on both the front and back for a total volume of 0.48cc based on a 4" wafer with 20% front coverage. Hence the materials cost is 5¢/wafer. Including overhead and an operator to monitor the process the total cost is expected to be 7¢/wafer.

2.3.5.4 Summary

The costs for the three metallization steps are summarized in Table 2.3.5.1

Equipment	
Silk Screening	0.01¢/wafer
Nickel Plater	0.02¢/wafer
Wave Soldering	0.03¢/wafer
Equipment Total	0.06¢/wafer
Materials	
Resist Ink	2.0 ¢/wafer
Screen and Stencil	0.8 ¢/wafer
Plating Solution	0.5 ¢/wafer
Solder	5.0 ¢/wafer
Material Total	8.3 ¢/wafer
Labor and Overhead	
Screen Printing Operator	3.0 ¢/wafer
Nickel Plating Operator	3.0 ¢/wafer
Wave Solder Operator	2.0 ¢/wafer
Labor and Overhead	8.0 ¢/wafer
Metallization Total	16.36¢/wafer

TABLE 2.3.5.1

3. Junction Formation, Quantum Yield

Verification of junction formation has essentially been completed. One particular measurement, however, was not finished in time for the last quarterly report. A measurement of quantum yield has been taken for textured 4" diameter cells diffused with spin-on dopants and is shown in Figure 3.1.1.

The quantum yield measurement is the ratio of charge carries generated in the external circuit to the number of photons absorbed. This is measured by illuminating the cell with spectrally narrow light. By knowing the wavelength and the intensity the number of incident photons per second can be derived. This value is compared to the number of generated charge carriers per second which is directly proportioned to the short circuit current. The ratio of incoming photons to short circuit current generated must be corrected for reflection losses. The curve, presented in Figure 3.1.1, takes this correction into account.

The spectral response of a textured cell formed with spin-on dopants compares well with cells whose junction is formed by gaseous diffusion.

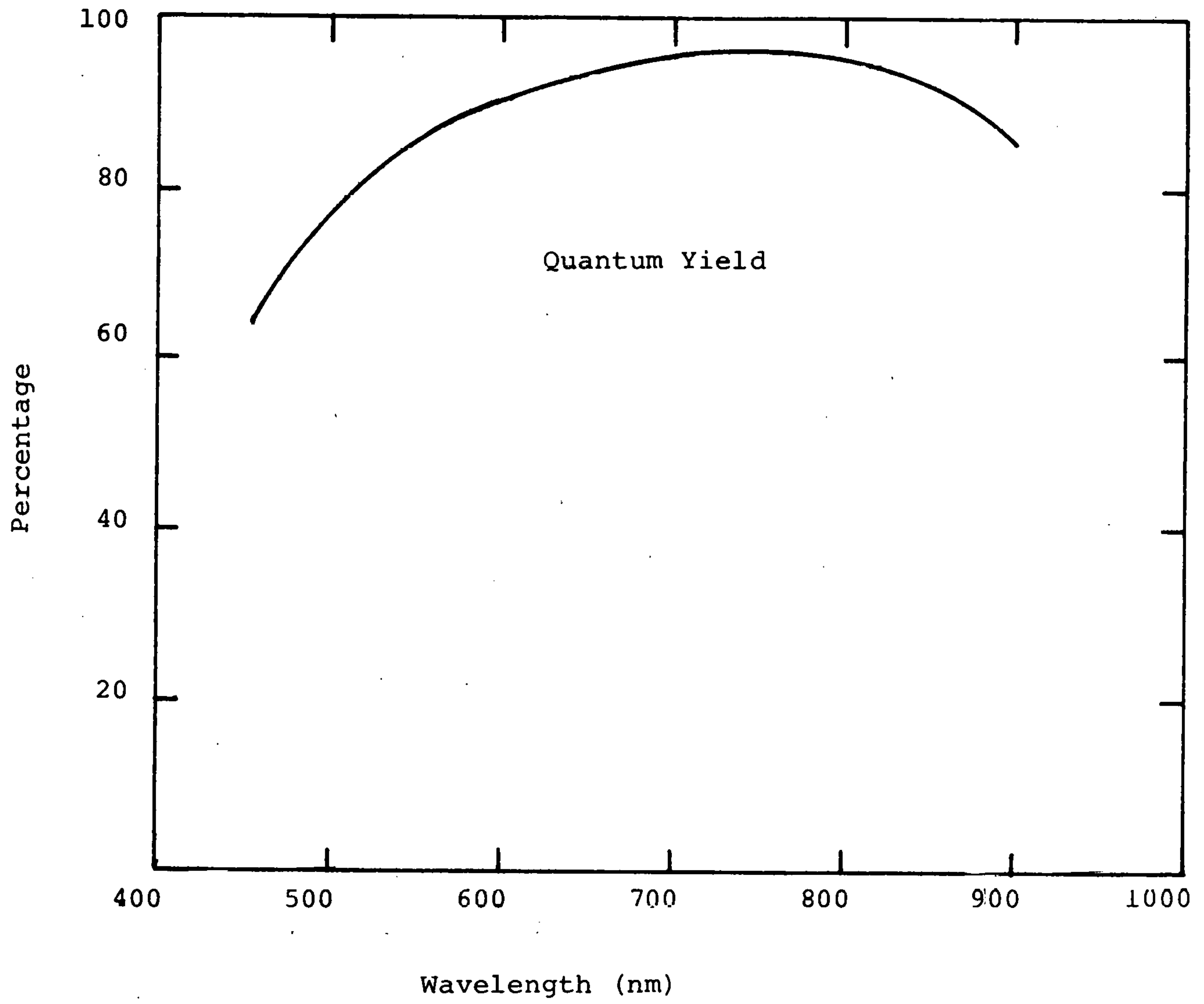

Figure 3.1.1 Quantum Yield for textured cell, Spin-on Dopant

4. Interconnection and Encapsulation

4.1 Review and Assessment of Interconnection and Encapsulation

Interconnection and encapsulation of solar cells onto panels can be accomplished in an efficient and automated fashion using our proposed lamination and reflow technique. Several parameters govern the production of these modules. A solar panel should, firstly, be cost effective using materials which are readily available and inexpensive. The entire process should lend itself to an automated sequence allowing smooth and efficient operation. Finally, material combinations must be found which withstand varying enviromental conditions to assure long panel life.

We will describe below how these parameters are met with our proposed sequence. We should emphasize, also, the process discussed in this section is not limited to one specific interconnection scheme. By varying the spray mask any possible arrangement of series and parallel connections can be obtained. All in all, our developing production techniques are characterised by great simplicity and flexibility for future automation.

4.1.1 Cost Effectiveness

In order that panel production cost be consistent with the national goal of $0.50/watt in 1986 each process must be carefully reviewed and verified. Panel fabrication has been designed to use readily available and inexpensive materials with a minimum of large equipment. Basic materials consist of glass, copper (in small quantity), and plastic. The actual amount of copper deposited on the glass is only a small percentage of the metal actually sprayed. The residual metal that is deposited on the mask can easily be scaped off and recycled aiding in making

the process less expensive. The use of glass as a superstrate material has been determined to be the most cost effective material available (approximately 4¢/wafer) for the production of solar panels. Likewise, lamination material consisting of a plastic which is produced in millions of pounds a year is not considered a large expense. In addition, the only major equipment required will be an arc sprayer , a press, wave solder machine and an oven. In the future, this apparatus will take over the entire encapsulation process eliminating the expense of human labor.

4.1.2 Ease of Automation

Ease of automation is a major consideration in selecting the proper process sequence. All of the steps should easily lend themselves to being placed in an automated environment.

An interesting possibility in this direction can be seen in using an arc sprayer to provide an interconnection scheme for solar panels. The arc sprayer is used to deposit a metal contact through a mask onto a sheet of glass. This machine can easily be operated in such a manner that sheets of glass could be coated in a continuous flow.

Once the contact pattern has been arc sprayed it is first wave soldered than a thin layer of plastic is applied to secure the solar cells in place. This layer can either be applied as a spray or as a thin sheet depending upon which materials are used. One can easily imagine a system whereby a plastic sheet (or spray) is applied to a pane of glass on a belt serving as an optical coupling to the cell. Likewise, the rest of the encapsulation sequence is specifically designed to be carried out in an automation fashion. A more detailed description of the proposal panel building process is presented later in this section where the ease of automation is demonstrated.

4.1.3 Environmental Stability

The life expectancy of a solar panel can be measured by its ability to withstand prolonged environmental exposure. A panel experiences a wide range of environmental changes including varying temperature cycles, rain, humidity and strong winds all of which cause the panel to stretch, contract, twist and bend. Under these stresses the panel should remain intact and it's output characteristics remain constant. We have chosen for panel building a lamination of glass and plastic that will withstand all these stresses.

As a superstrate, glass has a rigidity that is on par with silicon, and has demonstrated good environmental protection, and remains totally clear for decades. The plastic, which will bond the solar cells to the glass, is subject to various special parameters which restricts the number of suitable candidates. The material's susceptibility to ultraviolet degradation is of particular importance, hence UV stabilizing chemicals should be incorporated into the plastic if the glass does not act as a UV suppressing filter. The plastic should also be perfectly clear and adhere well to glass superstrate. The glass will protect the plastic from humidity and oxidation thereby eliminating synergistic effect when "the elements" work in conjunction with ultraviolet radiation. Depending upon the material's weatherability another layer of the same substance could be applied to the back, or a different type of plastic, or plastic and glass used which will totally seal off the panel. A review of the present work on lamination materials is presented in Section 4.2.2.

4.1.4 Encapsulation Sequence

Interconnection and encapsulation of solar panels is being developed towards a particular system but there remains some flexibility in a final choice of sequences. Techniques are being independently developed so that much can be learned about each individual process. Specifically these techniques are: 1) arc spraying 2) solder reflow, 3) lamination, and 4) parallel gap welding. The particular process which employs these methods starts with arc spraying a regular pattern of metal deposited throug a mask which will later serve as interconnects for the cells (Figure 4.1.4.1). The glass will be solder dipped to tin the interconnects. A thin layer of acrylic or other suitable plastic will be applied over the entire sheet which will later eliminate any air space between the cell and the glass providing also a good optical match. Solar cells are then positioned face down onto the arc sprayed electrode onto both the front of the cell and the soldered tab of the adjacent cell. An embossed plate will then be lowered onto the glass and moderate pressure applied to the cells and contacts. Infrared lamps will supply heat through the glass to the solder carrying contacts. The thin layer of acrylic will melt and the solder reflow establish contact of the arc sprayed electrode to both the front of the cell and the back tab of the adjacent cell.

Each individual process is undergoing verification work providing a great deal of flexibility in the final process steps.

4.2 Verification Experiments

4.2.1 Arc-Spraying

One of the prevailing methods of interconnecting cells utilizes hand soldering of metal tabs. One way to reduce costs is to mechanize the current tabbing procedure. We have

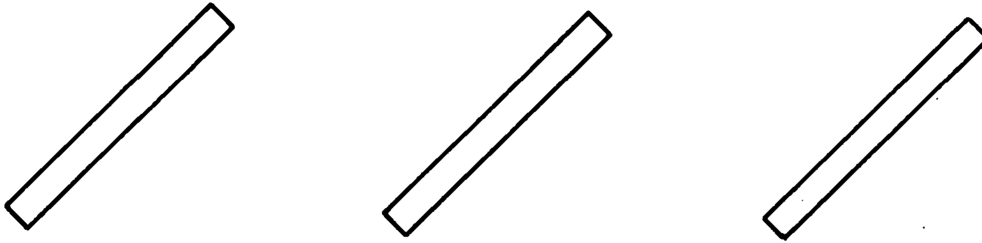

Arc Sprayed Contact Pattern On Glass, Enforced By Solder Dipping.

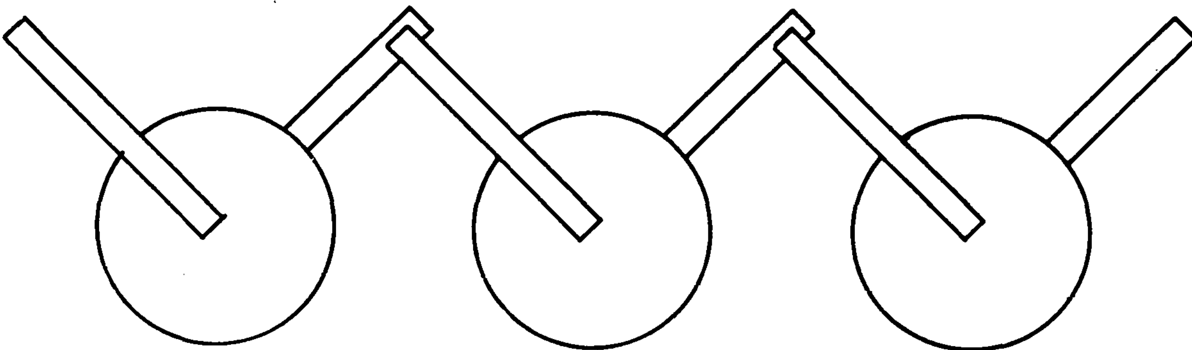

Cells Positioned Face Down With Their Back Contact Tab Overlapping The Front Contact Pattern Of Adjacent Cell.

(Simplest conceptual arrangement)

Figure 4.1.4.1

proposed an alternative approach in which the interconnection pattern is generated by spraying metal through a mask onto the glass superstrate of the panel. This alternative procedure has several advantages. First, the pattern is consistent from one panel to the next; once the spacing and conductor sizes have been established and a mask is made, each panel will faithfully reproduce the design. Second, when glass is used this technique is perhaps the simplest way to interconnect cells.

The metal is bonded to the glass by using an arc-sprayer. The operation of an arc-spaying machine utilizes an electric arc which is struck between two wires that are continuously fed towards each other. The molten metal from the wires is sprayed forward with a high velocity stream of air. Thousands of incandescent particles can be seen streaming from the nozzle. The heat and force of the spray depends on the distance between the nozzle and the workpiece. At distances greater than about eighteen inches the spray forms a powder that can be brushed away. Closer than three inches the spray can punch through sheet metal. At intermediate distances the spray becomes imbedded in the workpiece. Determining the proper distance (as well as air velocity and arc current) requires extensive experimentation.

We will now describe our experiments to date. We began by spraying onto glass through a sheet metal mask that delineated a pattern of tabs. It was found that copper generally does not stick to the glass. Under some conditions the copper adhered but the bonding strength was low.

In order to better understand the bonding process aluminum was tried next. Aluminum can be considered opposite to copper in two important properties. Aluminum bonds oxygen more readily

than silicon while copper bonds oxygen less strongly than silicon. This means that the aluminum is likely to chemically react with the glass, whose major constituent is silicon dioxide. Also, aluminum melts at the softening point of glass, around 660°C, while copper melts at 1083°C. The switch to aluminum proved to be fruitful as the deposited aluminum forms a layer that could not be removed by scraping.

In order to solder to the tabs copper was sprayed onto the aluminum. The copper bonded firmly to the aluminum. In turn, it was found that solder wetted the copper. This double spray step can easily be incorporated into an automated line.

In order to find the ultimate strength and the failure mode of the arc-sprayed contact a metal tab was soldered to the copper/aluminum/glass contact, then pull-tested. The contact pulled away from the glass at about 200 grams force leaving conchoidal fractures in the glass. This is shown in Figure 4.2.1.1 and 4.2.1.2.

Since the only failure observed was within the glass the bonding seems to be strong at all interfaces. The failure at 200 grams does not indicate a contact of lesser quality than standard tabbing procedure because the mechanical stresses are completely different. The only valid test is actual temperature cycling of laminated cells.

Future experiments will cover three areas: A broader spectrum of arc-sprayed metals including bronze, brass and iron; a complete investigation of spraying parameters (arc

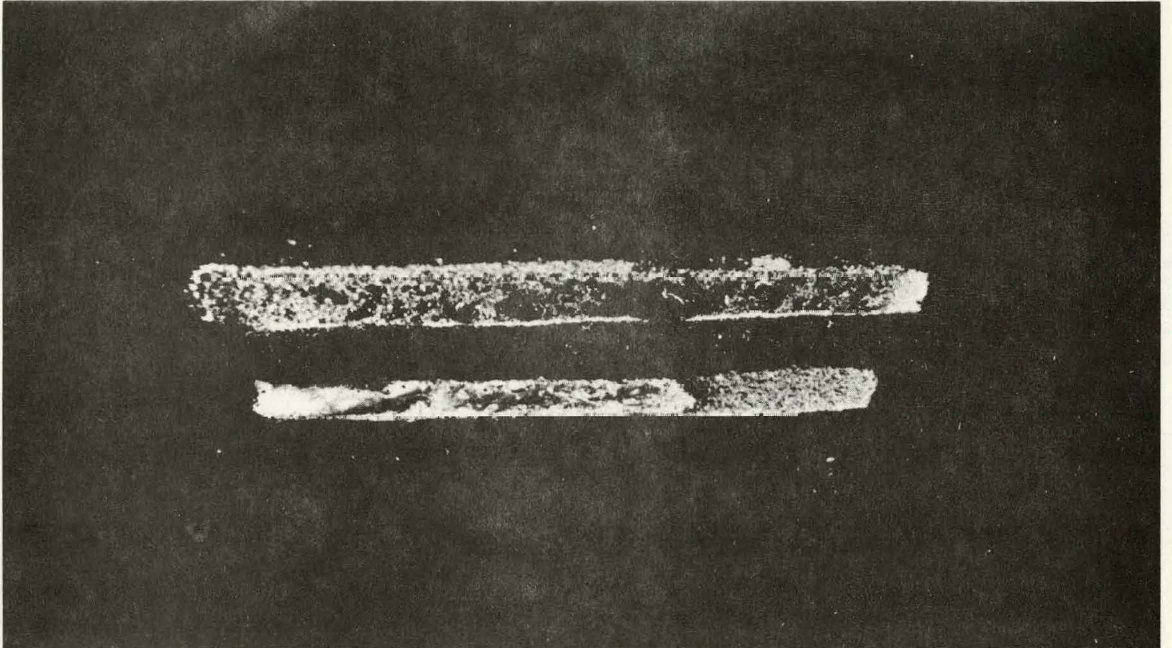

FIGURE 4.2.1.1

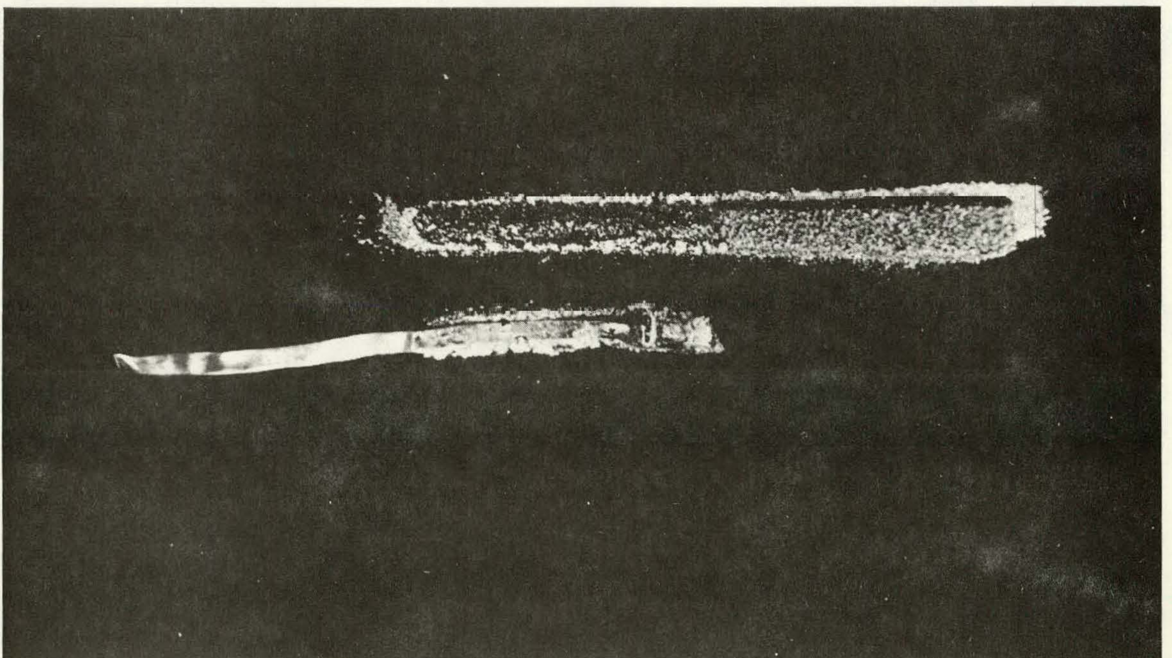

FIGURE 4.2.1.2

power, distance, air flow); and environmental testing of laminated cells.

In sum, arc-spraying is able to bond diverse materials quickly and simply. In particular, metal can be bonded to glass. This allows the interconnection step to be integrated with the encapsulation step with a savings in time and an assurance of uniformity. We are currently optimizing the procedure and anticipate that arc-spraying will be an important technique in panel building.

4.2.2 Laminating

A layer of clear plastic is placed between the cell and the glass to assure good optical coupling by eliminating the air gap. Further, the plastic absorbs stress generated by the different temperature expansion rates of the cell and the glass. The choice of plastic is constrained by several factors. First, the clarity and elasticity of the plastic must be retained for the life of the panel, at least twenty years. Second, the plastic must be suited to our proposed manufacturing technique involving lamination and solder reflow at an elevated temperature. Within these constraints a suitable group of plastic types can be chosen.

The environmental stability of plastics has been studied for years and the study of plastic behind glass is anticipated. It is appropriate, therfore, to begin our verification by looking at plastics under conditions that are unique to our proposed panel building sequence, that is, lamination and

solder reflow. Our first tests, began prior to installation of the arc-sprayer. Plastic films, and in one case a spray, were used to laminate a cell to glass. During the process the temperature was raised to 200°C since this temperature must be used to reflow the solder. Films of polyethylene, cellulose, acetate, polyester, and polyvinyl butyral; as well as acrylic spray have been tested. This covers a wide range of plastic families but stays within the bounds of low cost and ready availability.

Three types of plastic have shown promise: Poly-ethylene, polyvinyl butyral and acrylic. Our results are summarized in Table 4.2.2.1.

The time and pressure used in the lamination process varies from 10 to 60 minutes and 3-10 p.s.i. A much closer study of these two variables will be made when the solder reflow process is verified.

4.2.3 Parallel Gap Welding

Parallel gap welding has been employed in spacecraft solar arrays to interconnect cells for several years. The connections provide long life service to spacecraft for missions of many years. The welding equipment is readily available and easily adapted to automatic assembly fabricating techniques. Developments in this area have shown that the parameters of welding including voltage, time and force, can be chosen to provide good adhesion of the tab with the cell. Basically the process consists of providing a power discharge between two parallel electrodes in such a manner that it melts the materials together. Work done with the technique yielded

PLASTIC	Lamination Characteristics
POLYETHYLENE	Readily softens to form void-free interface. Self-cohesion greater than adhesion to glass.
CELLULOSE ACETATE	Yellows and becomes brittle.
POLYESTER	Does not soften sufficiently at 200°C.
POLYVINYL BUTYRAL	Very strong adhesion to glass and to silicon wafer. Readily absorbes water unless back of panel is moisture barrier such as glass.
ACRYLIC SPRAY (Dried before laminating)	Thick coat (.004") can be used to form void-free interface.

TABLE 4.2.2.1

results which are presented in Table 4.2.3.1. All of the samples were pulled at 45° and the welding parameters were as follows:

Weld Gap	15 mils
Voltage	1.1 volts
Weld Duration	9.0 ms
Tabbing Material	Tinned Copper
Cell Metallization	Ti-Pd-Ag

Figure 4.2.3.1 summarizes the results of the previous table in a histogram. One can see that the majority of samples withstood pull strengths of 600 grams and greater (mean pull strength: 689.7 grams) far exceeding the Air Force space cell specifications of 250 grams. The failure occured at the evaporated metal interface with the cell 98% of the time. In practically all instances the metallization parted from the cell before the tab parted from the metallization. It can be said, therefore, that the number presented here shows adhesion properties of the metallization rather than the tab weld.

Although our use of parallel gap welding proved successful it has been found that it might not be required. Wafers which emerge from the wave solder machine are coated with enough metal to allow soldering to the back. Soldering is a basic technique that requires only a few parameters for consistent success. In comparison with parallel gap welding soldering provides a good process which can be easily automated. Our welding results show good promise and can possibly be used in other areas of terrestrial photovoltaics.

Parallel Gap Welding Pull Strength Results

All Samples Pulled at 45°

Sample	Pull Strength (grams)	Sample	Pull Strength (grams)
1	339.6	36	778.3
2	707.5	37	948.1
3	452.8	38	382.1
4	495.3	39	608.5
5	580.2	40	424.5
6	721.65	41	792.4
7	452.8	42	226.4
8	608.5	43	566.
9	353.7	44	339.6
10	587.2	45	877.3
11	792.4	46	594.3
12	764.1	47	962.2
13	615.5	48	353.8
14	1018.8	49	452.8
15	551.9	50	566.0
16	608.5	51	622.6
17	268.85	52	594.3
18	438.7	53	495.2
19	382.1	54	735.8
20	877.3	55	962.2
21	509.4	56	424.5
22	353.75	57	268.9
23	438.7	58	566.
24	1061.3	59	580.2
25	792.4	60	141.5
26	700.4	61	650.9
27	679.2	62	735.8
28	863.2	63	665.1
29	792.4	64	509.4
30	1075.4	65	721.7
31	650.9	66	990.5
32	990.5	67	679.2
33	933.9	68	566.
34	689.2	69	608.4
35	636.8	70	735.8

Mean Pull Strength: 689.7 grams

Table 4.2.3.1

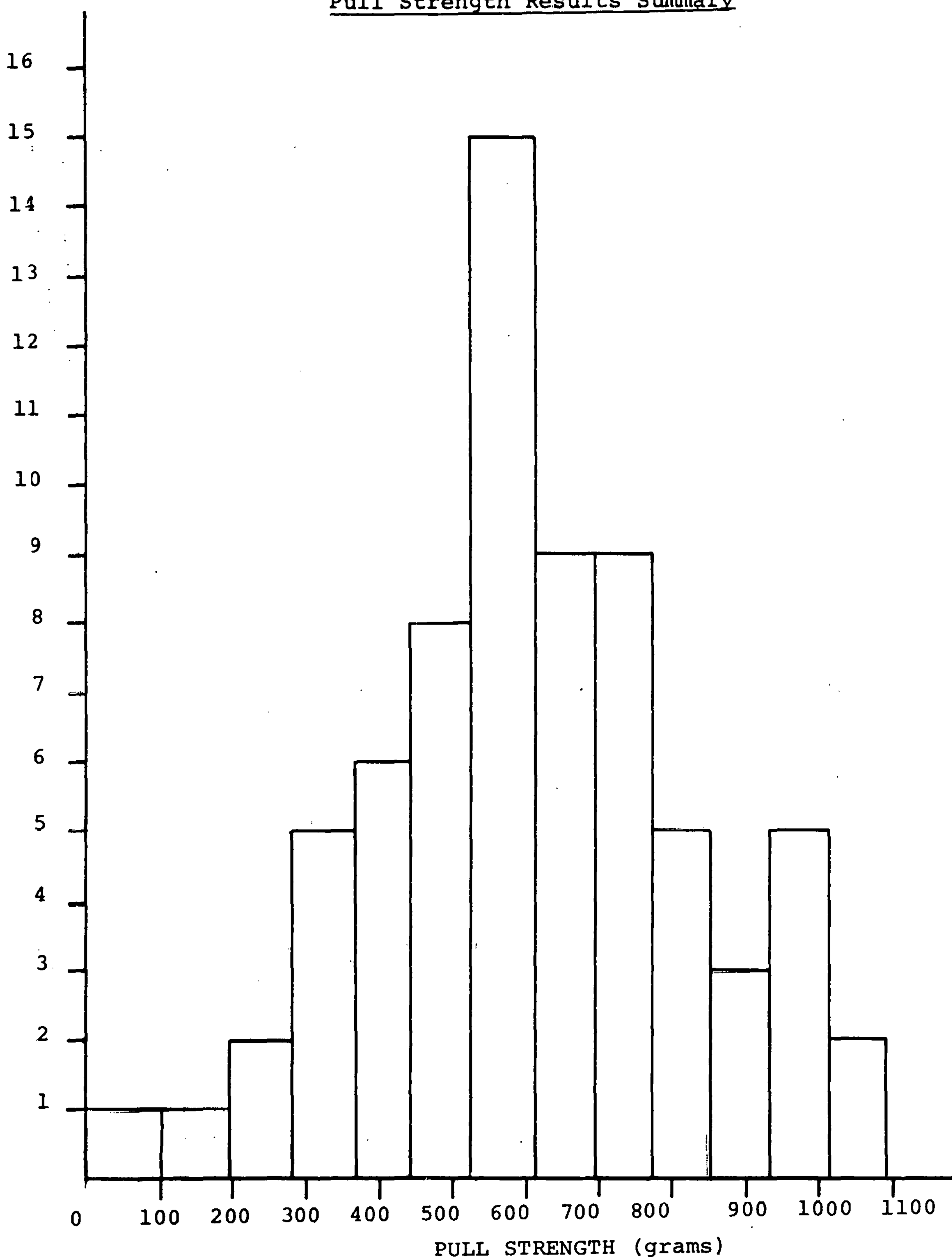

Figure 4.2.3.1

5. Conclusions

Our work up to this time has strengthened our beliefs that the process steps considered do lend themselves to automation and can be carried out economically so that the project goals can potentially be reached. The completion of the metallization work clearly demonstrates that our proposed sequence can meet the projected cost goals. In a similar manner, the interconnection and encapsulation of solar cells into modules shows great promise of being successfully completed as proposed. During the next quarter work will be directed towards arc-spraying and laminating. It is expected that a variety of materials will be tried in conjunction with varying process parameters in order to reliably produce panels in an automated fashion.

6. Recommendations

There are no specific recommendations at this time.

7. New Technology

There is no new technology to be reported during this quarter.

.S. GOVERNMENT PRINTING OFFICE: 1978-740-206/161